Buoyancy Driven Natural Ventilation through Horizontal Openings

Heiselberg, Per

Published in:
The Third International Workshop on Natural Ventilation

Publication date:
2009

Document Version
Publisher's PDF, also known as Version of record

BUOYANCY DRIVEN NATURAL VENTILATION THROUGH HORIZONTAL OPENINGS

Per Heiselberg, Prof., Ph.D.
Division of Architectural Engineering
Department of Civil Engineering, Aalborg University, Aalborg, Denmark

Abstract

An experimental study of the phenomenon of buoyancy driven natural ventilation through single-sided horizontal openings was performed in a full-scale laboratory test rig. The measurements were made for opening ratios *L/D* range from 0.027 to 4.455, where *L* and *D* are the length of the opening and the diameter of the opening, respectively. The basic nature of air flow through the single-sided openings, including air flow rate, air velocity, temperature difference between the rooms and the dimensions of the horizontal openings, were measured. A bidirectional air flow rate was measured using constant injection tracer gas technique. Smoke visualizations showed that the air flow patterns are highly transient and unstable, and that the air flow rate oscillates with time. Correlations between the Froude (Archimedes) number *Fr (Ar)* and the *L/D* ratio are presented. The correlation of *Fr* with *L/D* is reasonable agreement with Epstein's formula obtained from brine-water measurements, but the obtained *Fr* values show considerable deviations for a range of *L/D* ratios. Thus, revised formulas for natural ventilation are proposed.

Key words Natural ventilation, air flow rate, buoyancy, horizontal opening, tracer gas, LES

1. Introduction

Air flow through horizontal openings is an important issue of mass and energy transfer between different zones in buildings. Horizontal openings occur in staircases, stairwells, ventilation shafts, roof openings and chimneys. Air flow through vertical openings has been widely investigated but little is known about the flow in the horizontal openings, especially when they are driven by buoyancy (Shao, 1995).

Epstein (1988) has performed a detailed experimental study in a brine-water scale model for the exchange flow through a single horizontal opening in a large range of aspect ratios $0.01 \le L/D \le 10$. Epstein identified four distinct flow regimes as a function of aspect ratio. At very small opening heights ($L/D<0.15$) the pressure level on both sides of the opening is essentially the same and an oscillatory exchange flow regime will be established (Regime I). For larger values of *L/D* the flow regime changes from an countercurrent orifice flow regime (Regime II, $0.15 \le L/D \le 0.4$) to a turbulent diffusion flow regime for very large values (Regime IV, $L/D>3.25$). In the turbulent diffusion flow regime the air exchange was much slower and the countercurrent flow within the tube appeared to comprise of packets of warm and cold air with a chaotic and random motion. For intermediate values ($0.4 \le L/D \le 3.25$) the flow will be a combination of an orifice flow and turbulent diffusion flow regime (Regime III). According to the four flow regimes, Epstein gave the following relations between Froude numbers and *L/D* ratio:

$$Fr = \frac{q}{\sqrt{\frac{g(T_i - T_u)L^5}{T_i}}} \quad (1)$$

$$Fr = 0.055 \qquad \frac{L}{D} < 0.15 \quad (2)$$

$$Fr = 0.147\left(\frac{L}{D}\right)^{\frac{1}{2}} \qquad 0.15 < \frac{L}{D} < 0.4 \quad (3)$$

$$Fr = 0.093\frac{1}{\sqrt{1 + 0.084\left(\frac{L}{D} - 0.4\right)^3}} \qquad 0.4 < \frac{L}{D} < 3.25 \quad (4)$$

$$Fr = 0.32\left(\frac{L}{D}\right)^{-\frac{3}{2}} \qquad 3.25 < \frac{L}{D} < 10 \quad (5)$$

Where q is the exchange air flow rate [m^3/s], g is the gravitational acceleration [m/s^2], T_i is the inside temperature [K], T_u is the outside temperature [K], L is the length (or height) of opening [m] and D is the diameter of the opening [m].

Figure 1 shows the relations developed by Epstein for the four different flow regimes. The experimental results by Epstein as well as other authors are also included in the figure. It is seen that there are some deviation between equations (2) –

(5) and the experimental results, especially for flow Regime III, which is very relevant for natural ventilation openings in buildings.

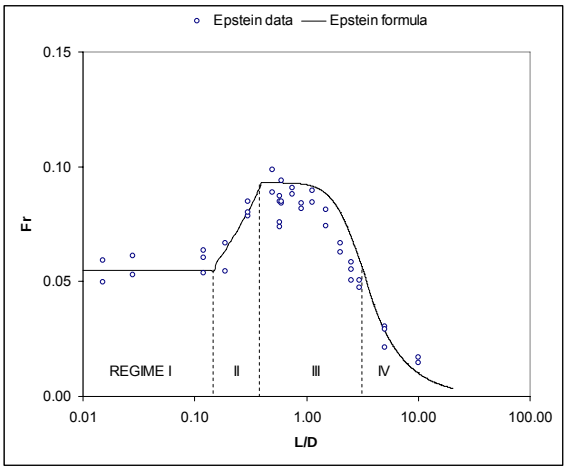

Figure 1. Experimental results for countercurrent exchange flow through a single opening, given by Epstein

This research work is focused on obtaining the air flow rate through the horizontal openings driven by buoyancy. The experimental analysis was carried out in a full-scale laboratory test rig. The basic nature of air flow through a single horizontal opening was measured. The measurement results can be used in both simple calculation tools to give a rough estimate of the capacity for design of a ventilation system, but also be implemented in more detailed models, especially multi-zone models, for simulation of the performance of natural ventilation systems.

2. Measurement Set-Up

The experimental analysis was performed in a laboratory of Indoor Environmental Engineering at Aalborg University. The essential features of the experimental system for the case of a single opening are schematized in Figure **2.**

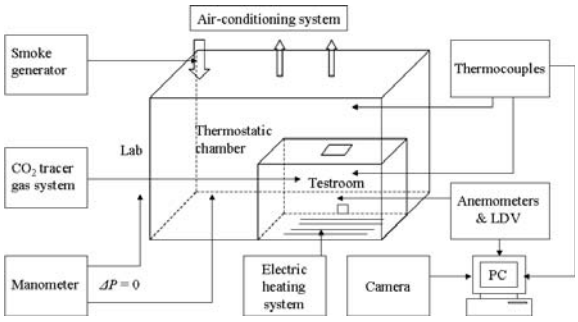

Figure 2. Schematic representation of system and measurement equipments.

A full-scale test cell which was divided into two rooms, namely the "thermostatic chamber" and the "testroom". The thermostatic chamber was 8 m length, 6 m width and 4.7 m height; and the testroom was 4.1m length, 3.2 m width and 2.7 m height, respectively. The thermostatic chamber simulated the environmental conditions controlled accurately by an air conditioner. Only one square horizontal opening was located on the roof center of the test room. The higher indoor temperature was produced by heating cables uniformly distributed on the floor inside the test room. CO_2 constant injection tracer gas system, thermocouples, anemometers and Laser Doppler Velocimetry (LDV) were used to measure the air flow rate, air temperatures and air velocities respectively. Special attention was paid to ensure the pressure difference to be zero between the chamber and the laboratory hall in order to avoid unnecessary errors of infiltration and exfiltration. Different cases were examined by varying the temperature differences of inside and outside of the testroom, the opening area and the opening ratio *L/D*. The measurements were carried out with a single square opening of side length 0.2 m, 0.4 m, 0.6 m, 0.8 m and 1.0 m, so the opening area varied from 0.04 m^2 to 1.0 m^2.

The roof thickness of the testroom is 0.13 m, and the opening height varied from 0.13 m to 1.0 m, thus the opening ratios *L/D* might vary in the range from 0.115 to 4.455. In order to measure the *L/D* ratios in the flow regime I, an insulated metal plate with thickness 0.012 m and side length 1.0 m was used and located on the test room roof center. A square hole was opened with different side length 0.1m, 0.2m, 0.3m and 0.4m, therefore the *L/D* ratios from 0.027 to 0.106 could be obtained for flow regime I. Because the square opening side length is smaller than the metal plate length, the flow influence of test room roof thickness may be ignored.

In this study only square openings were used. For a square opening with a side length *S*, *D* should be viewed as the diameter of a round opening that has the same area as the square opening described by the following relation:

$$D = \sqrt{\frac{4}{\pi} S^2} = 1.128 \cdot S \qquad (6)$$

The tracer gas system included injection and distribution devices, a flow meter and tracer gas sampling apparatuses. The average CO_2 concentration was measured after the tracer gas equilibrium state arrived and the opening was closed. According to the constant injection tracer

gas theory, the constant air flow rate at steady state can be obtained by the equilibrium concentration:

$$q = \frac{q_{tracer}}{C(\infty) - C(0)} \qquad (7)$$

Where q is the air flow rate [m^3/s], q_{tracer} is the tracer gas constant injection flow rate [m^3/s], $C(\infty)$ is the equilibrium concentration of the CO_2 tracer gas, $C(0)$ is the CO_2 concentration of the atmospheric air about 390 ppm.

When the equilibrium steady state was reached, a couple of fans were used to maintain homogenous mixing of the tracer gas in the room air and to measure the $C(\infty)$ after the opening was closed and the tracer gas supply stopped.

3. Air Flow Predictions by CFD

The bidirectional exchange of air through the horizontal opening was also predicted by CFD using the commercial CFD code FLUENT 6.1.18. Two three-dimensional turbulence models of standard k-ε model and LES model were simulated respectively.

Standard k-ε model with standard wall function

The governing equations solved by FLUENT include the three-dimensional time-dependent (or steady-state) incompressible Navier-Stockes equations and k-ε turbulence equations. For the k-ε turbulence equations, the empirical turbulence coefficients C_1, C_2, C_μ, σ_k and σ_ε are assigned the following values: C_1=1.44, C_2=1.92, C_μ=0.09, σ_k=1.0 and σ_ε=1.3. These values are widely accepted in CFD k-ε calculations. The pressure-velocity coupling was achieved using the PISO (Pressure Implicit with Splitting of Operators, Issa (1986)) algorithm. The second-order upwind differencing scheme was used to evaluate the convection terms for the Navier-Stokes equations, the energy equation and the turbulent transport equation, in order to reduce numerical diffusion.

The grid for the simulations consisted of approximately 410,000 computational cells, where high density grids were refined in the field around the horizontal opening. The standard wall functions approach was used in the *k-ε* turbulence model. A specified constant heat flux 20 W/m^2 through the test room floor was given to model the uniformly distributed heat source, and all the other walls were set to be adiabatic. The inlet boundary conditions of the thermostatic chamber were (given by measurement data): velocity 0.015 m/s, temperature 10 ºC, turbulence intensity 30% and turbulence length scale 0.1 m (Nielsen et al. 2003).

For the unsteady *k-ε* model CFD simulations, the first-order implicit unsteady formulation was used. The time step size Δt was set to be a proper value and the number of iterations converges to 10^{-3} at each time step. Thus, the number of iterations per time step is 10-20.

LES model with Smagorinsky-Lilly subgrid-scale model

The Reynolds stresses in Navier-Stockes equations can be modeled using the Samgorinsky-Lilly model in FLUENT (Smagorinsky 1963, Lilly 1966). This model uses a constant model coefficient C_s. Lilly derived a value of 0.23 for C_s from homogeneous isotropic turbulence in the inertial subrange. However, this value was found to cause excessive damping of large-scale fluctuations in the presence of mean shear or in transitional flows. C_s = 0.1 has been found to yield the best results for a wide range of flows. Therefore, this default value was used in LES simulations. The second-order central differencing scheme was used to discretize the convection terms. The pressure-velocity coupling was achieved using the PISO. The grid used in the LES simulations was the same with the grid used in *k-ε* simulations. Thus, the initial field of the LES can be obtained from the results of the *k-ε* simulation. The boundary conditions were similar with those used in the *k-ε* model.

For the LES simulations, the second-order implicit unsteady formulation was used. The time step size Δt was set to be a proper value and the number of iterations converges to 10^{-3} at each time step. The number of iterations per time step is 10-20. Since the LES runs a transient solution from the initial condition from the *k-ε* model results, the simulation must be run long enough to reach independence of the initial condition and to enable the statistics of the flow field.

The grid independence was tested for both models according to the air flow rate through the horizontal opening and further grid refinement yields only small and insignificant changes in the numerical results.

4. Results

Smoke visualization

The air above the opening has a lower temperature and a higher density and the air below the opening. The density difference creates a buoyancy driven down flow of more heavy air from the upper thermostatic chamber to the lower test room. Since the test room is sealed, mass conservation dictates

upflow of the lighter air. In the case of a single opening, this situation gives rise to bidirectional exchange flow across the horizontal opening.

In order to get a better understanding of this bidirectional flow, smoke visualizations were carried out. The air flow pattern in steady state near the opening was observed during the experiment. The smoke was introduced in the thermostatic chamber or in the testroom, thus the downflow or upflow was observed. Figure 3 shows the resulting downflow through the opening S = 0.4 m and L/D=0.295 at time t = 0.5 s, 1 s, 1.5 s and 3.5 s, respectively. The air velocity and airflow directions vary all the time through different part of the opening. The smoke visualizations showed that the bidirectional air flow is highly transient and unstable.

(A)

Figure 3 (C)

(B)

Figure 3 (D)

Figure 3. The smoke visualization of air downflow through the opening S = 0.4 m and *L/D*=0.295 at different time, (A) t =0.5 s, (B) t =1 s, (C) t =1.5 s and (D) t =3.5 s.

Laser doppler velocity measurement

Vertical velocity component measurements were performed using Laser Doppler Velocimetry (model: Dantec Flowlite laser-optics system). The experiment was made several times at different points at the opening for one case keeping constant temperature difference. Figure 4(A) presents the typical vertical velocity history during about 1000 seconds at the center point of the opening for case S = 1.0 m, L/D = 0.115, at temperature difference ΔT = 15 °C.

LDV measurements confirmed the qualitative flow patterns given by flow visualization, which means, the bidirectional flow is highly transient. The vertical velocity at one point varies quickly between positive (upflow) and negative (downflow). As a result the vertical component of flow measured by LDV can state the bidirectional flow motion and the spectral analysis of flow. The frequency of pulsations is measured from the power spectrum of LDV data. Figure 4(B) shows the corresponding spectrum at this center point, but the clearly defined frequency can not be

identified from the spectrum for this *L/D* aspect ratio.

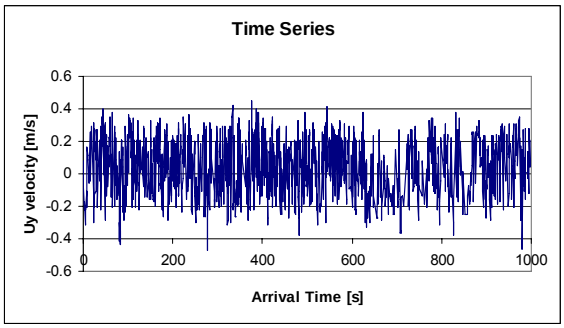

Figure 4(A) The vertical velocity history at the center point of the opening *S* = 1.0 m, *L/D* = 0.115, at temperature difference *ΔT* = 15.0 °C.

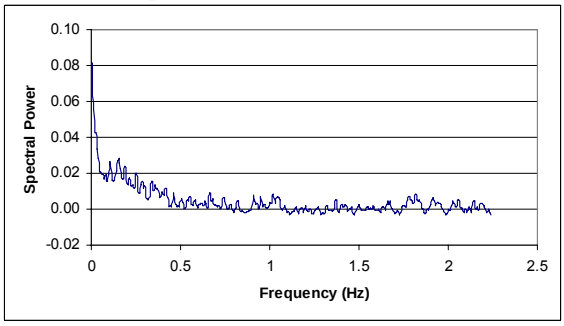

Figure 4(B) The corresponding spectrum at the center point of the opening *S* = 1.0 m, *L/D* = 0.115, at temperature difference *ΔT* = 15.0 °C.

Prediction of air velocities in the opening and the resulting air flow rate

The smoke visualization and velocity measurements show that the bidirectional air flow is highly transient and unstable. Therefore, the air flow rate oscillates with time and the measured air flow rate should represent a mean value.

Figure 5(A) and 5(B) show the air flow rate history calculated by time-dependent *k-ε* model and LES model. The time step size *Δt* was set to be 0.1s for *k-ε* model and 0.03s for LES. The calculated temperature difference between the test room and the thermostatic chamber is 15.3 ºC that changes slightly with the time. The measured air flow rate at this temperature difference is 27 m^3/h; and the calculated average air flow rate during the simulation flow time is 14.6 m^3/h for *k-ε* model and 29.2 m^3/h for LES model. The air flow rate calculated by LES agrees well to the measured data, whereas the air flow rate calculated by *k-ε* model is only about half of the measured value.

The steady state *k-ε* model was also simulated, but the converged solution could not be obtained since the buoyancy driven flow through this horizontal opening is highly transient and unstable. The time-dependent computation revealed that the flow patterns in the zones as well as in the horizontal opening are highly transient and unstable and the dominant mode of air exchange through the opening is intermittent pulses. The LES simulation gives the air flow rate pulse frequency about 0.3 s^{-1}, which is much higher than is given by the *k-ε* model.

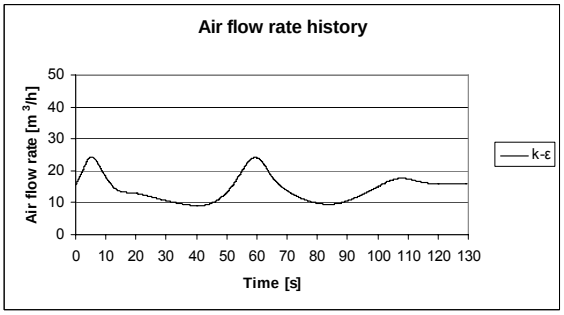

(A)

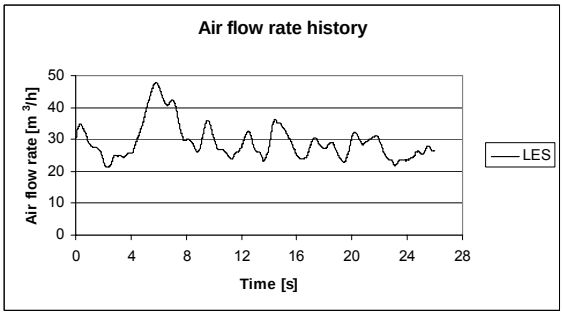

(B)

Figure 5. The air flow rate history for Case A of buoyancy driven natural ventilation through single-sided one horizontal opening, (A) calculated by *k-ε* model (B) calculated by LES model.

Figure 6 shows the air velocity vector distribution at the middle plane of the horizontal opening in X direction at four different time instants calculated by LES model. The flow pattern varies significantly between each time step.

Measured air flow rate at different opening areas and L/D ratios

Since the air flow across the opening is time-dependent, the air flow rates will oscillate with time and the measured "steady-state" air flow rate should be the mean value during a certain time period. For different measurement cases of different opening size and temperature differences, the injection period of CO_2 tracer gas varied from 2 hours to 2 days depending on the air flow rate value through the opening. Figure 7 shows the CO_2

concentration history at the center point of the testroom during the measurement case S = 0.8 m, L/D = 0.147, at temperature difference ΔT = 18.7 °C. Because the air exchange rate is quite small (or time constant quite large) compared to the volume of the test room the amount of tracer gas in the test room will only be affected marginally by the quick oscillations of the air flow rate in the opening and the concentration in the test room can be used to measure a reliable average value of the air flow rate.

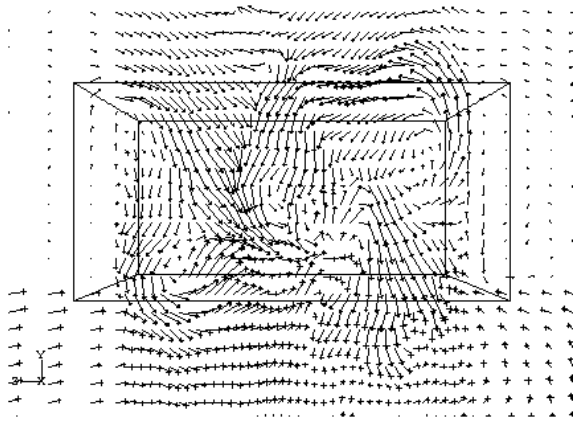

(A)

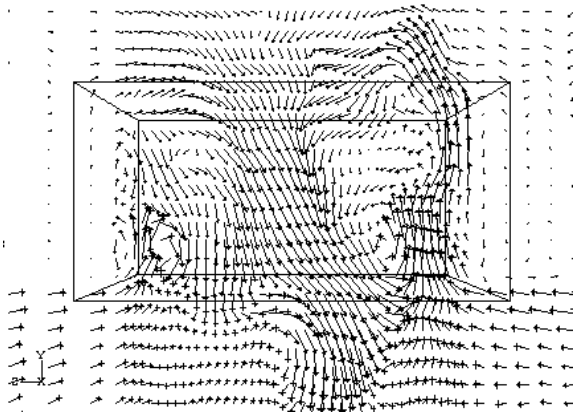

(B)

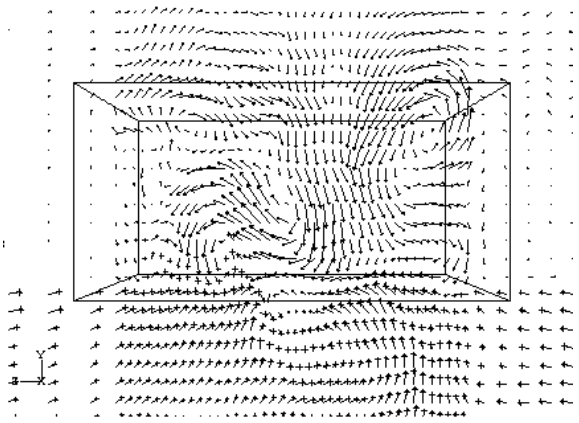

(C)

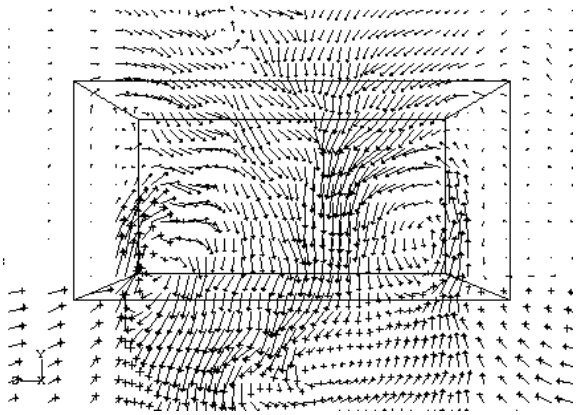

(D)

Figure 6. The air velocity vector distribution at the middle plane of the opening in X direction at four different time instants for Case A, (A) 11.3 s, (B) 12.5 s, (C) 13.7 s, (D) 14.6 s. calculated by LES model.

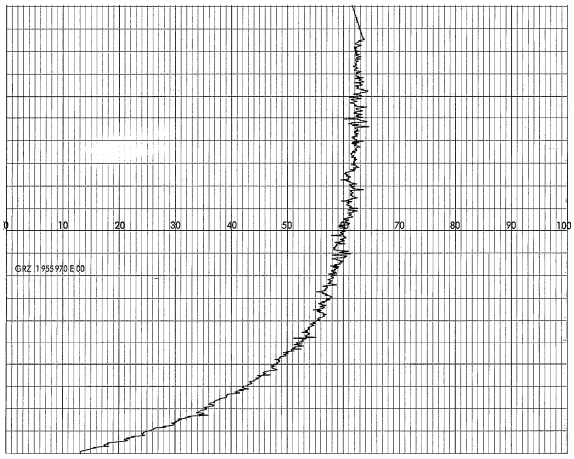

Figure 7. The CO_2 concentration history at the center point of the testroom for case S = 0.8m, L/D = 0.147, and ΔT = 18.7 °C.

Figure 8(A) and (B) shows air flow rate versus temperature difference for different flow regimes and compares measured data with the calculated data from Epstein's formula. For a certain opening configuration the air flow rate increases as the temperature difference increases because of higher buoyancy driving force. Generally, the deviations between the measured data and the Epstein's formulas increase when the temperature difference increases. The air flow rate also changes significantly in the horizontal openings with different L/D ratio. In some cases the measured air flow rates fit quite well with the Epstein's formula, such as the case of L/D = 0.295, S = 0.4 m in flow Regime II; but in some cases the measured data show clear deviations from the Epstein's formula,

such as the case of $L/D = 1.108$, $S = 0.8$ m in flow Regime III. For example in Figure 8(B), the flow rates estimated by Epstein formula have no significant differences when L/D changes from 0.443 to 1.108, while the experimental measurement indicates that the air flow rates vary significantly at these L/D ratios.

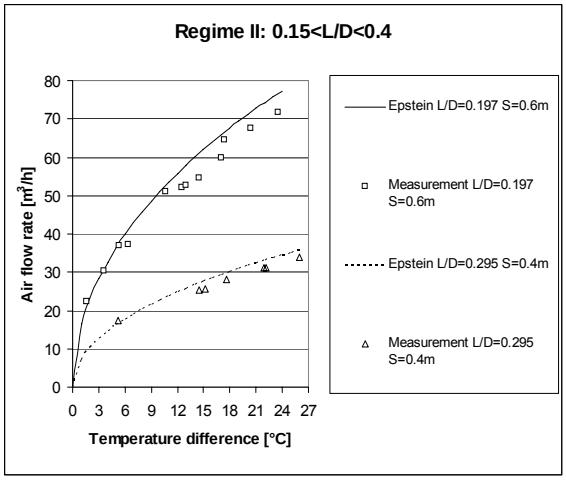

(A)

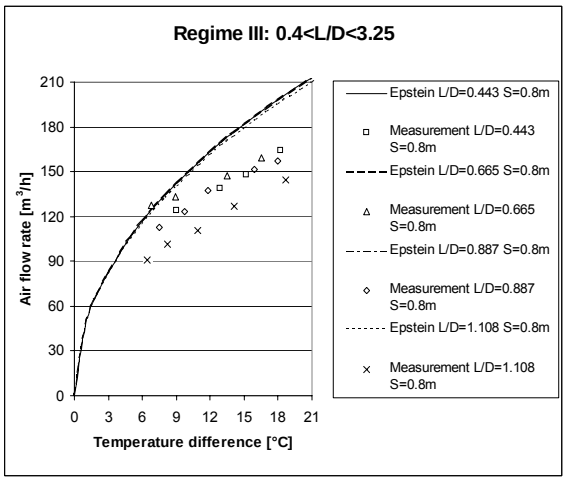

(B)

Figure 8. The comparisons of air flow rate versus temperature difference in different flow regimes between the measured data and the calculated data from Epstein's formula.

In order to compare the full-scale air flow measurement data with the Epstein's brine-water scale-model measurement data all the data are represented as Froude numbers versus L/D ratios in figure 9. Although the full-scale measurement data in general fit well with the results from the brine-water scale measurements significant differences exist between them.

For opening ratios L/D from 0.035 to 0.115, the dimensionless air flow rate Fr was found to be about 0.050, which is lower than the constant Fr value of 0.055 given by Epstein. Conover et al. (1995) as well as Sandberg and Blomqvist (2002) also found values lower than 0.055. Their values were between 0.035 and 0.047. When the L/D ratios are 0.027 and 0.03, the Fr are about 0.067 which is much higher than 0.055. The large deviations in this situation is probably influenced by the test room roof thickness, since the opening side length of 0.35 – 0.4 m is not much smaller than the hole's side length 1.0m.

The maximum dimensionless air flow rate was found to be about 0.11 for $L/D = 0.59$ in stead of $L/D = 0.4$, and approximately 15% higher than the peak value of 0.095 predicted by Epstein.

From the dimensionless Fr curve in Figure 9 it can also be seen, that only three flow regimes can be identified in this experimental study: Oscillatory exchange flow (Regime I), Bernoulli flow (Regime II), and turbulent diffusion (Regime IV). The combined turbulent diffusion and Bernoulli flow (Regime III) was not very clear in this figure.

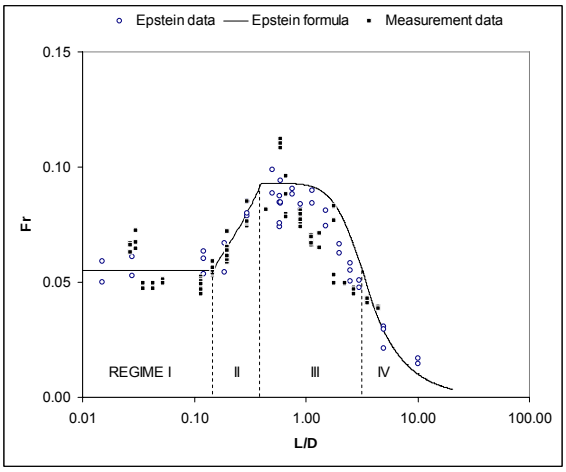

Figure 9. The *Fr* comparison between the full-scale air flow measurement and the Epstein brine-water scale measurement.

Proposal for revised formulas

According to the above data analyses, a revised proposal for the relation between air flow rate (Fr) and opening configuration (L/D) can be derived. The Fr value in the experimental study at L/D range below 0.115 can be expressed as:

$$Fr = 0.050 \qquad \frac{L}{D} < 0.115 \tag{8}$$

Since the measurement data fit the Epstein's formula quite good in the opening ratio L/D range

from 0.115 to 0.55, the *Fr* value at *L/D* range from 0.115 to 0.55 can be expressed as:

$$Fr = 0.147\left(\frac{L}{D}\right)^{0,5} \qquad 0.115 < \frac{L}{D} < 0.55 \qquad (9)$$

The major difference in the *Fr* value was found when the *L/D* range from 0.4 to 2.7. The combined turbulent diffusion and Bernoulli flow (Regime III) and turbulent diffusion (Regime IV) may be defined by using only one formula as:

$$Fr = 0.077\left(\frac{L}{D}\right)^{-0,5} \qquad 0.55 < \frac{L}{D} < 4.455 \qquad (10)$$

The comparison between the Epstein's formulas and the proposed revised formulas can be seen in Figure 10.

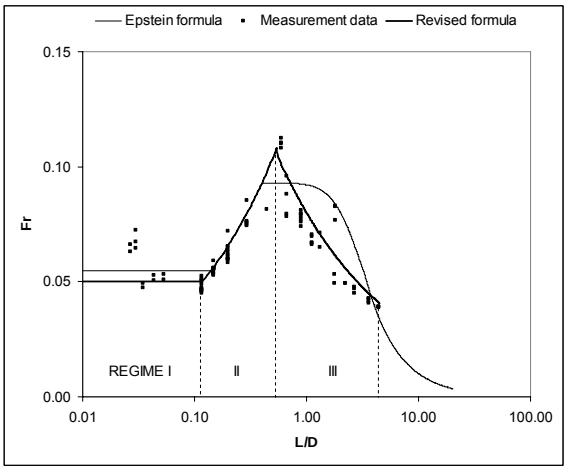

Figure 10. The dimensionless number *Fr* comparison between the Epstein's formula and the developed formula.

Conclusions

The highly transient, unstable and complex phenomenon of buoyancy driven natural ventilation through single-sided horizontal openings was investigated in order to deepen understanding of the character of air flow within buildings. This study has been focused on the bidirectional exchange flow through a single opening.

Based on the experimental results a revision of the Epstein's formulas for estimating the air flow rate is proposed. The revised formulas are useful for prediction of the air flow rate of buoyancy driven natural ventilation through a single horizontal opening. The limitation in this study is that only a maximum *L/D* ratio 4.455 was investigated and configurations outside this range need further studies. More measurements will also be required for *L/D* ranges below than 0.035, since significant deviations were found in this situation, probably due to the laboratory set-up.

The air flow rate and air flow pattern were predicted by the *k-ε* model and LES model. The LES model agree well with the measured data, while simulations by the *k-ε* model were inaccurate compared to the measured data. The *k-ε* model simulation requires less computing time than the LES, and it can provide detailed airflow field distribution. However, the predicted ventilation rate and the air flow field could be wrong due to the simplification of the method for the highly transient and unstable flow in the investigated case. The LES model seems to be a suitable tool to study natural ventilation by providing detailed and accurate air flow information.

References

Blomqvist C. and M. Sandberg, A Note on Air Movements through Horizontal Openings in Buildings, 8th International Conference – Air Distribution in Rooms, ROOMVENT 2002, Copenhagen, Denmark, 2002.

Conover T. A., R. Kumar and J. S. Kapat, Buoyant Pulsating Exchange Flow through a Vent. Journal of Heat Transfer, vol. 117, 641-648, 1995.

Epstein M., Buoyancy-Driven Exchange Flow Through Small Openings in Horizontal Partitions, J. Heat Transfer, vol. 110, 885-893,1988.

Issa R.I., Solution of implicitly discretized fluid flow equations by operator splitting. J. Comput. Phys., 62, 40-65, 1986

Lilly D.K. On the application of the eddy viscosity concept in the inertial subrange of turbulence. NCAR Manuscript 123, 1966

Nielsen P.V., S. Murakami, S. Kato, C. Topp, J.-H. Yang, Benchmark tests for a computer simulated person, ISSN 1395-7953 R0307, 2003

Shao L. and S. B. Riffat, CFD Investigation of Unstable Airflow due to Temperature Difference via Horizontal openings, Proceedings of the Second International Conference: Indoor Air Quality, Ventilation and Energy Conservation in Buildings, vol. 1, 419-427, Montreal, Canada, 1995.

Smagorinsky J. General circulation experiments with the primitive equations. Monthly Weather Review 91, 99-165, 1963.